Article

Not peer-reviewed version

A LiDAR-Based Method for Incorporating Foliar Biomass in Aboveground Carbon Estimates in Tropical Forest Enrichment Plantations

Stephane Takoudjou Momo *, Achille Biwole, Pauline - Andrée Medou Me Ze, Hermann Kondjio, Stephane Tchakoudeu, Yanick Serge Nkoulou, Bonaventure Sonké, Jean-Louis Doucet

Posted Date: 23 March 2026

doi: 10.20944/preprints202603.1717.v1

Keywords: AGB allocation; LiDAR; allometry; uncertainty; tree architecture; tropical forests; Congo basin

 doi:10.20944/preprints202603.1717.v1

Article

A LiDAR-Based Method for Incorporating Foliar Biomass in Aboveground Carbon Estimates in Tropical Forest Enrichment Plantations

Stéphane Takoudjou Momo [1,2,3,*], Achille Biwolé [4], Pauline - Andrée Medou Me Ze [1,5], Hermann Kondjio [4], Stephane Tchakoudeu [5], Yanick Serge Nkoulou [6], Bonaventure Sonké [2] and Jean Louis Doucet [1]

[1] Forest Is Life, TERRA Teaching and Research Centre, Gembloux Agro-Bio Tech, University of Liège, Passage des Déportés 2, 5030 Gembloux, Belgium
[2] Plant Systematic and Ecology Laboratory (LaBosystE), Department of Biology, Higher Teachers' Training College, University of Yaoundé I, P.O. Box 047, Yaoundé, Cameroon
[3] Congo Basin institute, University of California, Los Angeles, Los Angeles, CA, USA
[4] Laboratory of Forest Resources and Wood Valorisation, Advanced Teacher's Training College for Technical Education, The University of Douala, P.O. Box. 1872, Douala, Cameroon
[5] Pallisco SARL, Avenue des Cocotiers 478, BP 394, Douala, Cameroon
[6] Association Technique Internationale des Bois Tropicaux, Cameroon
* Correspondence: takoudjoumomo@gmail.com

Abstract

Accurately quantifying aboveground biomass (AGB) in tropical forests remains challenging, particularly in regenerating stands where tree crown architecture, size structure, and species composition strongly diverge from those used to calibrate classical allometric equations. Here, we evaluate whether leaf biomass typically ignored in LiDAR workflows can be predicted and improve AGB estimation derived from LiDAR data. We combined destructive measurements on 83 trees with high-resolution Mobile LiDAR Scanner (MLS) point clouds to quantify biomass. We also calibrate leaf mass models and assess the contribution of foliar biomass to total AGB. Stems accounted for most biomass (65%), while leaves contributed only 3% on average. Among models tested, the model 3, integrating DBH, projected crown area and wood density showed the best adjustment (R^2 = 54.4%; RMSE = 2.43 kg). This model outperformed both regional (-20.4%) and pantropical (-25.6%) allometric equations. This work highlights the importance of canopy features in forest carbon assessments and refines the use of LiDAR data as a robust alternative for estimates and monitoring AGB across tropical forests.

Keywords: AGB allocation; LiDAR; allometry; uncertainty; tree architecture; tropical forests; Congo basin

1. Introduction

Tropical forests exhibit extraordinary structural and functional complexity; driven by the diversity of life forms and ecological processes they host (Hallé et al., 1978; Poorter et al., 2006). Tree morphology or architecture, liana-laced canopies, and multilayered understories make them not only among the most beautiful ecosystems on Earth, but also among the most ecologically vital. They host over two-thirds of the planet's terrestrial biodiversity and play a central role in stabilizing global climate systems (Bonan, 2008). They are particularly effective for carbon sinks or stock, storing around 55% of all carbon in forest biomass, mostly in the aboveground compartments of trees (Bastin et al., 2018; Hubau et al., 2020; Pan et al., 2011). But as vital as they are, these ecosystems are also fragile, under diverse pressures such as deforestation, degradation, and climate shifts (Mitchard,

 doi:10.20944/preprints202603.1717.v1

2018; Siyum, 2020). Monitoring their fitness and accurately quantifying their biomass has never been more urgent (Duncanson et al., 2021). Biomass, and in particular aboveground biomass (AGB), is not just a static number or proxy, it is a living metric of forest function, resilience, and contribution to global carbon balance. For decades, researchers have relied on allometric equations, developed from destructive harvesting, to estimate this biomass (Brown et al., 1989; Chave et al., 2005). These equations relate diameter of breast height (DBH, in cm), tree height (H, in m), and wood density (WD, in $g.m^{-3}$) to AGB (Chave, 2005; Chave et al., 2014; Djomo et al., 2010; Djomo and Chimi, 2017; Dorisca et al., 2011; Fayolle et al., 2018; Ngomanda et al., 2014). While widely used and undeniably valuable, these models have clear limitations: i) they are often based on restricted datasets and rarely reflect the full diversity of tropical forests, ii) two trees that share the same DBH may exhibit different AGB (Molto et al., 2013); and iii) they can only be applied in natural forest, since the tree architecture could be different in planted forests or agroforestry systems. Applying them broadly can result in biases (Chave et al., 2014; Goodman et al., 2014; Molto et al., 2014; Ploton et al., 2016), especially in forests undergoing active regeneration or management forest (Feldpausch et al., 2012; Jucker et al., 2017). Although these limitations are well known, only a few studies have empirically quantified their potential impact. Goodman et al. (2014), reported that pantropical equations could underestimate AGB by up to 46% in dense tropical forests due to architectural variations. Similarly, Ploton et al. (2016) showed that errors linked to crown architecture could lead to biomass estimation differences exceeding 30%, especially in structurally complex stands. These findings highlight the critical need for alternative or complementary AGB descriptors beyond DBH and height, particularly those that capture crown structure (Lines et al., 2022). Yet, despite this scientific evidence, studies that have leveraged destructive data to validate such alternatives are very scared.

This last decade is characterised by a quiet and amazing revolution of some data such LiDAR in forest or ecological science (Disney, 2019). Terrestrial laser scanning (TLS) or mobile laser scanning (MLS) which are ground-based LiDAR technologies, are changing the game on how we observe and understand forests (Disney, 2019; Lines et al., 2022; Malhi et al., 2018). Rather than relying solely on indirect measurements like DBH, these technologies capture the detailed three-dimensional structure of trees and forests, down to the curvature of branches and the shape of crowns (Disney et al., 2018; Hackenberg et al., 2015; Lines et al., 2022; Malhi et al., 2018; Raumonen et al., 2013; Terryn et al., 2020, 2023; Verbeeck et al., 2019). These technologies generate dense point clouds that can be converted into quantitative structure models (QSMs), which estimate the volume of woody components with unprecedented precision (Åkerblom et al., 2017; Burt et al., 2019; Hackenberg et al., 2015a; Kaasalainen et al., 2014; Raumonen et al., 2015, 2012). When combined with species-specific wood density values, these QSMs offer direct or non-destructive estimates of AGB (Calders et al., 2015; Disney, 2019; Disney et al., 2019)or help to build new allometry equations (Gonzalez de Tanago et al., 2018; Lau et al., 2019; Momo Takoudjou et al., 2018; Muledi et al., 2025). Across tropical forests, TLS-derived estimates have shown exceptional agreement with destructive sampling, offering new levels of spatial accuracy and structural realism (Burt et al., 2021; Calders et al., 2015; Demol et al., 2022; Gonzalez de Tanago et al., 2018; Hackenberg et al., 2015b, 2014; Momo Takoudjou et al., 2018; Vandendaele et al., 2024). But, perhaps more importantly, TLS and MLS are bridging scales. They could help to ground-truth and calibrate satellite missions like NASA's GEDI and ESA's BIOMASS, linking tree-level measurements with forest-wide carbon maps (Duncanson et al., 2021; Réjou-Méchain et al., 2019; Sagang et al., 2024). Yet even this revolution has its blind spots. One of the most overlooked components in current biomass estimation workflows is the leafy part. QSMs, powerful as they are, were designed for conversion of woody part into cylinders or volume. Leaves, with their thin, complex and often overlapping structures, are typically filtered out during processing and more generally trees were scanned without leaves. These can constitute a significant fraction of total AGB, especially in young tropical trees or regenerating forests. Studies have reported that leaf mass accounts for approximately 2% to 15% of aboveground biomass depending on species, forest type, and tree size class (Kenzo et al., 2010; Kossi Ditsouga et al., 2024; Salis et al., 2006). As a result, most TLS or MLS-based biomass estimates only account for stems and branches, implicitly assuming that

 doi:10.20944/preprints202603.1717.v1

the leafy component is negligible, probably because: i) the huge work existing on leaf/wood segmentation (Matheus B. Vicari et al., 2019; Wang et al., 2020); ii) few studies have had the data needed to test whether it's possible to predict leaf biomass without trying to model each leaf. But what if we could estimate leaf mass not by separating it from wood, but by looking at something more holistic, based on crown shape?

Crown architecture has long been recognized as a key functional trait (Díaz et al., 2016; Osnas et al., 2013; Verbeeck et al., 2019; Wright et al., 2004). Traits like projected crown area, crown depth, and height-to-diameter ratio (H/D), or others are associated with species strategies for light interception, mechanical stability, and competitive success (Jackson et al., 2019; Jucker et al., 2025, 2022; Lines et al., 2022). These traits are not only easy to derive from 3D LiDAR data, but they are routinely measured in trait ecology and functional biogeography (Lines et al., 2022). Large global databases such as *Tallo* have begun compiling crown trait data across forest types, highlighting their ecological significance (Jucker et al., 2022). Their use in predicting leaf biomass derived from 3D data has remained virtually unexplored largely due to a lack of destructive reference data.

This leads to the central question of our study is it possible to predict more accurately the AGB of enrichment plantings (or regenerating forests) by computing a equation which incorporate the leaf mass? To answer this, instead of trying to process leaf-wood segmentation, we focused on whole-crown geometry. Hence, this study is about more than just improving biomass models, it's about rethinking the way we see trees. Trees are not just trunks and branches. They are organisms shaped by light, wind, and time (Jackson et al., 2019; Lines et al., 2022). The aim of this study is to assess whether crown shape metrics derived from mobile LiDAR can be included in models or workflow to accurately estimates AGB in regenerating forests. This study should thus contribute to increasing research efforts that bridge gaps between structural measures and functional processes in tropical forest ecosystems.

2. Materiel et Methods

2.1. Study Area

The study was conducted in southeastern Cameroon in the Eastern region of Cameroon (between 3°01′ N and 3°44′ N; 13°20′ E and 14°31′ E), more specifically in the forest management units (FMUs) 10-030, 10-042, and 10-044, managed by Pallisco-CIFM. The region belongs to the Guineo-Congolian semi-deciduous moist forest, dominated by species from Malvaceae and Cannabaceae (Droissart et al., 2023; Letouzey, 1985; Réjou-Méchain et al., 2021; White, 1983). Climate is equatorial with two rainy seasons, annual rainfall of 1,300–1,800 mm, and mean temperature ~24 °C (Fayolle et al., 2013). Elevation ranges between 600–760 m on ferrallitic soils (Jones et al., 2013). Our sampling was carried out in enrichment plantations established by Pallisco-CIFM as part of its regeneration program. Because these plantations represent early stage, rapidly changing forest structure, they provide an ideal setting to test whether LiDAR-based approaches, especially those accounting for foliage reduce biases in AGB estimation. So, measurements were performed in enrichment plots established since 2008 and installed in open secondary forests. In these plots, after marking large-diameter trees (> 60 cm) and commercial species, the undergrowth was cleared using machetes or bulldozers. Subsequently, nursery-grown seedlings of timber species were planted at a spacing of 3 × 3 m. The planted species alternated in groups of 25 seedlings (15 × 15 m) or in lines (for a detailed description, see (Doucet et al., 2016).

2.2. Data Collection

2.2.1. LiDAR Acquisitions

Between December 2023 and January 2024, 19 plots ranging from 0.2 to 1.6 ha were scanned using the handheld mobile laser scanner GeoSLAM ZEB-HORIZON (MLS) (see Appendix 1: Table 1). This single-return instrument operates at a wavelength of 903 nm, captures approximately 300,000

 doi:10.20944/preprints202603.1717.v1

points per second, and integrates 16 sensors (Bauwens et al., 2016; Proulx et al., 2022). It provides a maximum range of 100 m with an accuracy of 6 mm, operating at 10 Hz and covering a 360° × 270° field of view (Vandendaele et al., 2022). Prior to each acquisition, a rapid clearing was performed to reduce occlusion and allow us to easily move between each different plantations block. Two white reference spheres were systematically placed at the plot origin to facilitate subsequent processing, enabling both the identification of the starting point and automatically alignment the point cloud to the geographical north. Unlike earlier MLS models, our MLS directly integrates co-registration step during acquisition, producing a complete 3D point cloud at the end of each survey using the GeoSLAM algorithm. Each plot was selected based on following criteria: (i) plantation age (4-15 years), (ii) planting configuration (block or row planting) and (iii) plot preparation (manual and bulldozer) (see Appendix 1).

Table 1. Families and species destructively sampled, including scientific and commercial names, number of tree sampled (n), range of diameters (DBH in cm), mean wood specific gravity (in g.cm^{-3}) from the global database (WSG), and species guilds.

Family	Genus	Species	Com. name	n	DBH	H	WSG	Guild
Combretaceae	Terminalia	superba	Fraké	18	[6.7–33.9]	[4.55–22.36]	0.459	P
Fabaceae	Bobgunnia	fistuloides	Pao rosa	7	[5.2–22]	[6.33–16.5]	0.866	P
	Cylicodiscus	gabunensis	Okan	6	[5.9–14]	[4.41–9.16]	0.790	P
	Pterocarpus	soyauxii	Padouk	3	[5.9–8.6]	[4.11–7.1]	0.658	NPLD
Malvaceae	Mansonia	altissima	Bété	12	[5.9–23]	[6.62–15.1]	0.564	NPLD
	Triplochiton	scleroxylon	Ayous	15	[5.7–30.7]	[5.06–24.63]	0.334	P
Meliaceae	Entandrophragma	utile	Sipo	6	[5.2–9]	[4.91–6.69]	0.537	NPLD
Ochnaceae	Lophira	alata	Azobé	8	[8.1–32]	[7.13–14.27]	0.897	P
Sapotaceae	Baillonella	toxisperma	Moabi	8	[5.5–13]	[5.2–11.04]	0.725	NPLD

2.2.2. Destructive Sampling

Between March and May 2024, 83 trees from 9 species and 6 families were felled across different plots age previously scanned (Table 1). These species represent a wide range of structural and functional strategies, covering pioneers (P) as well as non-pioneer light-demanding (NPLD) guilds. The dataset encompassed between 6 and 17 individuals per species, with diameters at breast height (DBH) ranging from 3.76 to 34.26 cm and total heights between 4.1 and 22.4 m. Wood specific gravity (WSG) spanned from 0.334 g·cm^{-3} in *Triplochiton scleroxylon* (Ayous) to 0.897 g.cm^{-3} in *Lophira alata* (Azobé), thus capturing a large gradient of mechanical and ecological strategies. The selection includes both widespread timber species (e.g., *Terminalia superba*) and high-value hardwoods (e.g., *Baillonella toxisperma*, *Bobgunnia fistuloides*), providing a representative basis for evaluating crown metrics, leaf biomass allocation and allometric variability in Guineo-Congolian forests or enriched areas.

Before felling, DBH was measured at 1.3 m or above the last stem irregularity and total height was determined using a Haglöf Vertex V hypsometer (Fayolle et al., 2018). After felling, trees were divided into three vertical compartments: (1) stump, which is the part of the stem below the felling cut; (2) stem corresponding to the merchantable section of the tree bole; and (3) crown which encompasses all living branches and foliage above the main stem. Stump and stem volumes were obtained through log cubage, while crown components were carefully separated into branches and leaves before weighing. This log cubage consists of to divide the stem into 1-m logs from the stump

 doi:10.20944/preprints202603.1717.v1

up to the base of the live crown. The last segment was measured up to the first major branch insertion, so that the entire commercial bole was fully covered (Fayolle et al., 2018). For every 1-m log *i*, we measured the over-bark diameters at the lower and upper ends (D_{1i} and D_{2i}, in cm) using a diameter tape, as well as the log length L_i (in m) with a measuring tape. The volume of each log was then computed using Smalian's formula (1):

$$V_i = \frac{\pi}{8} \times L_i(D_{1i}^2 + D_{2i}^2) \quad (1)$$

where diameters were converted from centimetres to metres before calculation, and V_i is the log volume in cubic metres. Total stem volume was obtained by summing the volume of all 1-m logs along the bole (2):

$$V_{stem} = \sum_{i=1}^{n} V_i \quad (2)$$

Stump volume was computed in the same way, treating the stump as an additional short log between ground level and the felling cut.

Fresh leaves and twigs ≤ 1 cm were weighed with electronic balance with 0.01 g precision and subsamples were preserved in airtight bags for laboratory analyses. They were then oven-dried at 60 °C and reweighed until a constant weight (*i.e., <1% variation between two weighing 6 h apart)* was reached, following the protocol of Sirri et al. (2019). The total tree leaf mass (TLM, in kg), representing dry leaf biomass, was estimated by correcting the fresh leaf mass of each tree for its species-specific average moisture content (Eq. 3). The latter was calculated as the mean moisture content of subsamples collected per species.

$$TLM_{i,j} = FLM_{i,j} \times \left(1 - \frac{MC_j}{100}\right) \quad (3)$$

where, $FLM_{i,j}$ is fresh leaf mass of individual i of species j, MC_j is moisture content of species j compute as follows: ($\frac{1}{n}\sum_{i=1}^{n}(\frac{FMs_{i,j} - DMs_{i,j}}{FMs_{i,j}} \times 100)$ (4)). $DMs_{i,j}$ and $FMs_{i,j}$ are the dry and fresh mass of leaves respectively. The measured stump and stem volume were converted into aboveground biomass (AGB, in kg) using a wood density (WD, in g.cm^{-3}) value, corresponding to the species-level averages reported in the Global Wood Density Database (Zanne et al., 2009). The resulting stump and stem biomass (AGB_{ss}) were then summed with $TLM_{i,j}$ to obtain the destructively derived tree aboveground biomass (AGB_{Dest}).

2.2.3. LiDAR Point Cloud Processing and Structural Attribute Extraction

After the automatic co-registration performed in the GeoSLAM software, trees were extracted using a semi-automatic approach following the procedure described by (Martin-Ducup et al., 2021). This process involved (Appendix 2: Figure 1): (i) matching inventory data with the point cloud, (ii) individually isolated each tree, and (iii) segmented wood and leaves components using LeWoS (Wang et al., 2020). For more details about this procedure pleased refer to Martin-Ducup et al. (2021). Structural metrics including diameter at breast height (DBH, cm), total height (H, m), and crown attributes such as projected crown area (PCA, m²) were extracted from each point cloud using the ITSMe R package (Terryn et al., 2023) (Figure 1). Tree Quantitative Structural Model (TreeQSM) algorithm was subsequently applied to the woody point clouds, after which the optimal QSM was retained (Raumonen et al., 2013). This QSM was then manually refined in AMAPstudio-Scan to correct any remaining mis-fitting issues, following the workflow described by Momo Takoudjou et al., (2018). Finally, aboveground biomass (AGB_{MLS}) derived from MLS, were obtained by converting QSM volume into biomass using a WD derived from dryad database (Calders et al., 2015; Demol et al., 2021a; Raumonen et al., 2013; Zanne et al., 2009).

 doi:10.20944/preprints202603.1717.v1

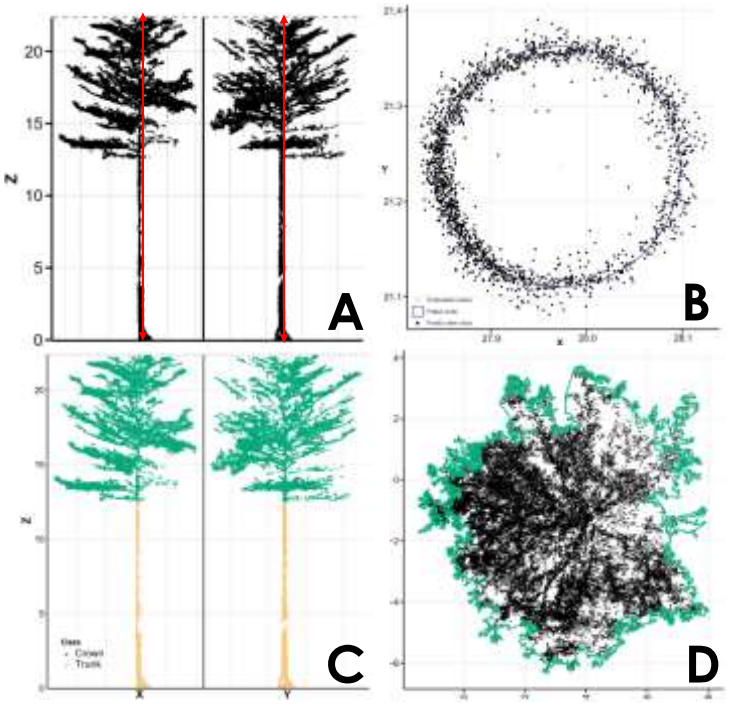

Figure 1. Main steps illustrating measurements of structural and crown metrics extracted from tree points cloud. A) Tree height measurement. B) Diameter at breast height (DBH) through circular fitting of a stem cross-section). C) Trunk and crown segmentation. D) Projected crown area (PCA) derived from the horizontal projection of the crown points on the ground plane.

2.2.4. Data Analysis

Preliminary data exploration has included descriptive statistics and distribution checks for all structural and biomass variables. Relationships between destructively measured parameters (leaf mass, total AGB) and LiDAR-derived metrics were assessed using Pearson's correlation coefficients. Secondly, we tested whether AGB allocation among tree compartments varied among species. For this, we summed, for each species, the total dry biomass of stems (which includes stump and bole), branches and leaves and build a species-compartment contingency table (9 species × 3 compartments). We also applied a Pearson chi-square (χ^2) test (*using a chisq.test function R*) whether the relative contribution of each compartment to AGB depended on species. A significant χ^2 value was interpreted as evidence that AGB allocation among stem, branch and leaf compartments is species-dependent. A set of predictive three models was developed to estimate total leaf biomass from structural attributes such as projected crown area, height-to-diameter ratio and crown depth.

$$\text{m1}: \ln(TLM) \sim \beta + \alpha_1 \times \ln(DBH) + \varepsilon \quad (4)$$

$$m2: \ln(TLM) \sim \beta + \alpha_1 \times \ln(DBH) + \alpha_2 \times \ln(PCA) + \varepsilon \quad (5)$$

$$\text{m3}: \ln(TLM) \sim \beta + \alpha_1 \times \ln(DBH) + \alpha_2 \times \ln(PCA) + \alpha_3 \times \ln(WD) + \varepsilon \quad (6)$$

where, TLM (kg) represents the destructively measured leaf biomass, DBH (cm) is the diameter of breast height, PCA (m^2) is the projected crown area and WD (kg/m^{-3}) is the species wood density which derived from dryad database. β *and* α are the model coefficients, and ε is the residual error term, assumed to follow a normal distribution. Model selection followed an information-theoretic approach using the Akaike Information Criterion (AIC) and the coefficient of determination (R^2) and the residual standard error (RSE) to identify the best-performing predictors (Table 2). Model accuracy was assessed using the root mean square error (RMSE, in kg) defined as:

$$RMSE = \sqrt{1/n \sum_{i=1}^{n} \left(TLM_i - TLM_{ip}\right)^2} \quad (7)$$

 doi:10.20944/preprints202603.1717.v1

where TLM_i and TLM_{ip} denote the observed and predicted values of total leaf biomass, respectively. However, log-transformation introduces a systematic bias when data are back-transformed, a correction factor (CF) was applied, defined as CF = exp (RSE²/2), where RSE represents the residual standard error of the model (Chave et al., 2014; Fayolle et al., 2018). Additional k-fold cross-validation at the tree and species levels further demonstrated the robustness of the model (Momo et al., 2020). Finally, the AGB estimates derived from MLS data that explicitly included leaf biomass ($AGB_{MLSLeaf}$) were compared with those obtained from MLS without leaves (AGB_{MLS}), as well as with destructive AGB and those derived from two reference allometric equations: the regional model of Fayolle et al. (2018), and the pantropical model of Chave et al. (2014). We quantified the deviation of each AGB estimate from the destructive reference (AGB_{obs}) using two complementary metrics: the bias (B, in %) and the relative error (S, in %). B and S were calculated as follows:

$$B = \left((\bar{\hat{y}} - \bar{y})/\bar{y}\right) \times 100 \qquad (8)$$

where $\bar{\hat{y}}$ and $\bar{y}$ are average of predicted and observed AGB values.

$$S = \left((\hat{y} - y)/y\right) \times 100 \qquad (9)$$

where $\hat{y}$ and y are of predicted and observed AGB values. All data analyses were carried out in R (version 4.5.0;Team, 2025), with an alpha risk level of 0.05 for statistical significance.

Table 2. Linear models developed to predict tree leaf dry mass (Msf, kg) derivred from LiDAR data. Models were fitted using the natural logarithm of structural variables including diameter at breast height (DBH, cm), projected crown area (PCA, m²), and wood density (WD, g·cm⁻³). Parameter estimates (a, b, c, d) are presented with standard errors (±SE). Model performance metrics (R^2, RSE, AIC, RMSE) are reported to assess model fit and predictive accuracy.

Models	Model parameters				Model Perforrmance			
	a (±)	b (±)	c (±)	d (±)	R2	RSE	AIC	RMSE
m1 : ln(**Msf**) ~ a + b×ln(**DBH**)	-2.96***(0.46)	1.53*** (0.19)	-	-	48.19	0.780	179.49	2.63
m2 : ln(**Msf**) ~ a + b×ln(DBH) + c×ln(**PCA**)	-2.67*** (0.45)	1.12*** (0.24)	032* (0.12)	-	52.52	0.752	174.94	2.53
m3 : ln(**Msf**) ~ a + b×ln(DBH) + c×ln(PCA) + d×ln(**WD**)	-2.57*** (0.45)	1.15*** (0.24)	0.36** (0.12)	0.48. (0.28)	54.37	0.742	173.96	2.43

significance levels indicated by asterisks (*** p < 0.001, ** p < 0.01, * p < 0.05).

3. Results

3.1. Leaf Mass Contribution to Total Aboveground Biomass

Across the full dataset (n = 83), the chi square (χ^2) test revealed a highly significant species effect on biomass partitioning among stem, branches and leaves (χ^2 = 102.7, df = 16, p < 0.001). The Pearson residual heatmap (Figure 2a) shows that these differences are driven by a few notable deviations from the overall pattern. *Lophira alata* allocates substantially more biomass to the stem and less to branches than expected under independence, whereas *Mansonia altissima* and *Triplochiton scleroxylon* display the opposite trend, with a higher-than-expected branch contribution and a reduced stem share. *Entandrophragma utile* combines relatively high stem and leaf fractions with a deficit in branches, while the remaining species lie close to the expected values (residuals ≈ 0). Overall, these results indicate that, beyond the general dominance of stem biomass, species differ significantly in how they distribute AGB among structural compartments. The stacked barplot in Appendix 3 (Figure 2) summarises the mean biomass partitioning pattern for each species. In all cases, stems account for the largest share of AGB (≈60-80%), branches contribute 20-40%, and leaves remain a minor component (<7%). However, some species depart from this average structure: *Lophira alata* and *Entandrophragma utile* show relatively higher stem fractions, while *Mansonia altissima* and *Triplochiton scleroxylon* allocate a larger proportion of biomass to branches, in line with the χ^2 residual patterns (Figure 2a). This global view of biomass partitioning across for example DBH classes and functional guilds confirms the patterns observed at the species level. For the full dataset, stems systematically dominate AGB (65-71%), with branch biomass ranging between ~28 and 41%, and leaves remaining

 doi:10.20944/preprints202603.1717.v1

a small but non-negligible fraction (2-7%) with slightly higher proportions in small trees (Appendix 2 Figure 2). Small trees (<10 cm DBH) show reduced stem contribution and proportionally more branches and foliage, whereas larger trees (>30 cm DBH) invest more strongly in the stem compartment. Differences between non-pioneer light-demanding and pioneer species are modest: pioneers allocate slightly more biomass to stems (66% vs. 61%) and slightly less to branches, while leaf proportions remain consistently low in both guilds (Figure 2b). This both guilds allocate their AGB in very similar proportions with no significant difference (see Appendix 4 Figure 3).

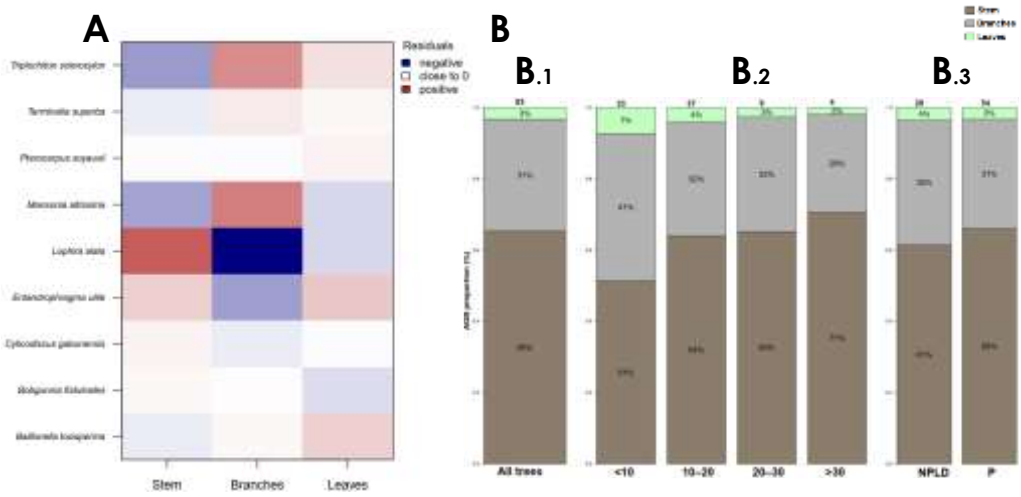

Figure 2. Aboveground biomass among tree compartments. A) Pearson residuals from the χ^2 test of independence between species and biomass compartment. Colours represent the sign and magnitude of deviations from the expected frequencies: dark blue cells indicate compartment under-represented for a given species, white cells no deviation and dark compartment over-represented. B) Across diameter classes and functional guilds (B.1) for all trees, (B.2) according to diameter class and (B.3) regarding to species functional guilds (non-pioneer light-demanding and pioneer only). Compartments are stem, branches and leaves and the number of trees sampled in each group is given on top of each bar.

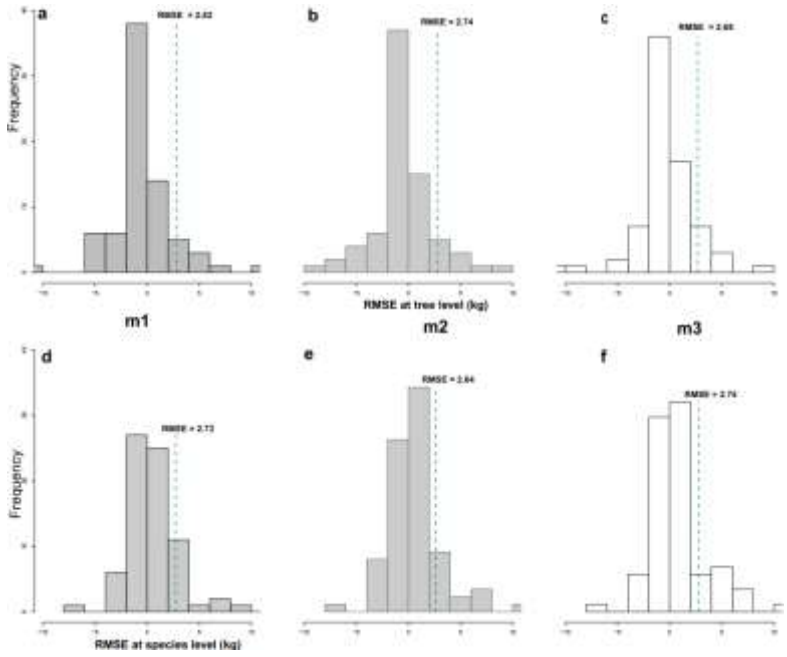

Figure 3. Frequency distributions of tree (a–c) and species (d–f) levels of root mean square error (RMSE, in kg) showing the distribution of RMSE for the three models of leaf dry mass (Msf) during cross-validation. Dashed vertical lines represent the mean value for each model.

 doi:10.20944/preprints202603.1717.v1

3.2. Model Calibration and Validation Based on MLS Metrics

Among the three log-log models calibrated for predicting total leaf mass (TLM), the first model with DBH-only showed the weakest performance (Table 2). Although it explained 48.19% of the observed variability with R^2, its uncertainty remained high, as reflected by both residual and prediction errors (RSE = 0.83; RMSE = 2.77). Incorporating projected crown area (PCA) improved predictive model performance, an increased explanatory variability (R^2 = 52.52%), and slightly reduced AIC and RMSE values, indicating a more efficient description of TLM. The full model which includes DBH, PCA, and wood density (WD), showed the agreement with destructive measurements, with tighter prediction and the highest explained variance (R^2 = 54.37%). This model also achieved the lowest AIC (173.96) and RMSE (2.43), demonstrating greater accuracy.

Cross-validation conducted at individual (a-c) and species (d-f) scales demonstrated strong model stability: prediction errors remained tightly closed to zero and aligned closely with calibration errors, indicating limited overfitting and robust generalization (Figure 4). At the individual scale, RMSE values ranged from 2.68 to 2.82 kg across models, indicating stable and reliable predictions of total leaf mass (TLM). At the species scale, RMSE values showed a similar pattern, reflecting moderate interspecific variability but no substantial loss of predictive accuracy. Overall, these results highlight the consistency and robustness of all three models across hierarchical levels, with only limited propagation of prediction error from individual trees to species-level estimates.

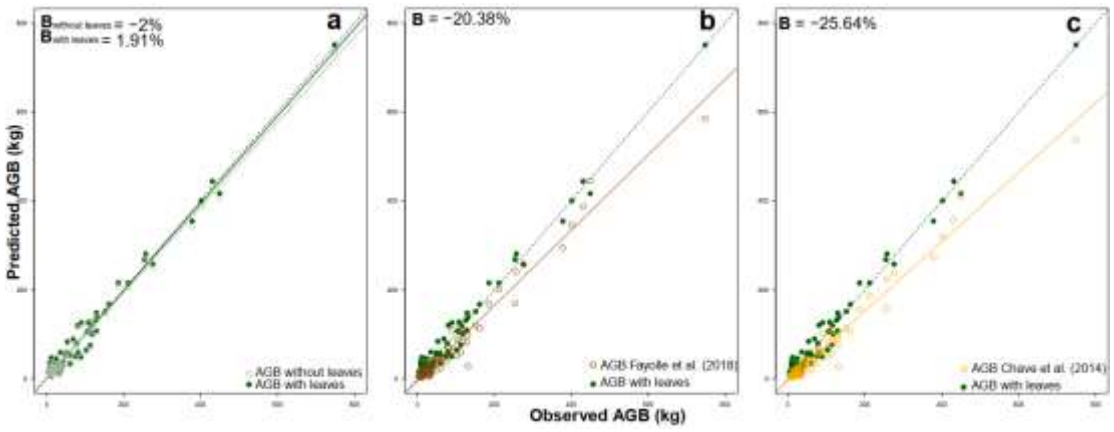

Figure 4. Comparison between observed aboveground biomass (AGB) and predictions from MLS-derived estimates (with and without leaf biomass) and from reference allometric models. Panels: (a) MLS-based AGB with and without leaf biomass; (b) AGB predicted using the regional allometry of Fayolle et al. (2018); (c) AGB predicted using the pantropical model of Chave et al. (2014). For each panel, the 1:1 line is shown as a black dashed line, solid-colored lines represent model fits, and the corresponding bias values are reported in the upper-left corner.

3.3. Tree Level Biomass Estimations

Based on the cross-validation results, we selected model 3 (m3) to predict total leaf mass (TLM). These TLM predictions were then added to the traditional tree AGB ($AGB_{observed}$) estimates obtained by multiplying total wood volume by species wood density. Across the three comparisons, the inclusion of foliar biomass improved the goodness of fit between MLS-derived AGB estimates and destructive measurements (Figure 4). For MLS-based AGB, predictions excluding leaves showed a slight underestimation (Bias = -2%), whereas integrating leaf mass produce an opposite estimate (Bias = +1.91%), with points aligning closely along the 1:1 line (Figure 4a). When we compared MLS-derived AGB with the regional allometric model of Fayolle et al. (2018), the direct, tree-specific volume estimates obtained from MLS clearly outperformed the regional allometry. Fayolle et al. (2018) equation showed a strong systematic underestimation in these enrichment plantations (Bias = -20.38%), whereas MLS-based estimates that combine measured volumes with species wood density were much closer to the destructive observations (Figure 4b). A similar pattern has founded with

 doi:10.20944/preprints202603.1717.v1

pantropical equation of Chave et al. (2014), which showed even larger negative bias (-25.64%), especially for medium and large trees (Figure 4c). In both allometric comparisons, MLS with explicit foliar mass consistently tracked the destructive AGB more accurately than the reference allometries. Overall, this explicitly modelled foliage component has further reduced the remaining disparity, but the main improvement over regional allometry comes from using directly measured volumes rather than a generic DBH-height-WD relationship.

Given that the accuracy of AGB predictions can be strongly size-dependent, we explored how relative errors (S in %) behave across our DBH spectrum and how MLS-derived estimates compare to classical allometric models. This S obtained with our m3, regional and pantropical allometries varied strongly with tree size, revealing a clear DBH-dependent bias in AGB predictions (Figure 5). For small trees (DBH < 8 cm), both models exhibited large deviations, but in opposite directions, AGB MLS-derived estimates (m^3) overestimated AGB, whereas the Chave et al. (2014), equation systematically underestimated it. For intermediate diameters (10-30 cm), MLS predictions were close to zero error, indicating nearly unbiased estimates, while allometric predictions remained consistently negative (-20 to -40%), reflecting a persistent structural underestimation. For larger trees, both approaches converged toward moderate error levels, but MLS estimates remained consistently closer to zero, showing reduced systematic bias compared to the allometric model. Overall, these results demonstrate that when considering the TLM derived from point clouds improves AGB estimations, accuracy and bias across the tree size gradient, particularly for small and mid-sized trees where conventional allometric equations show their greatest limitations.

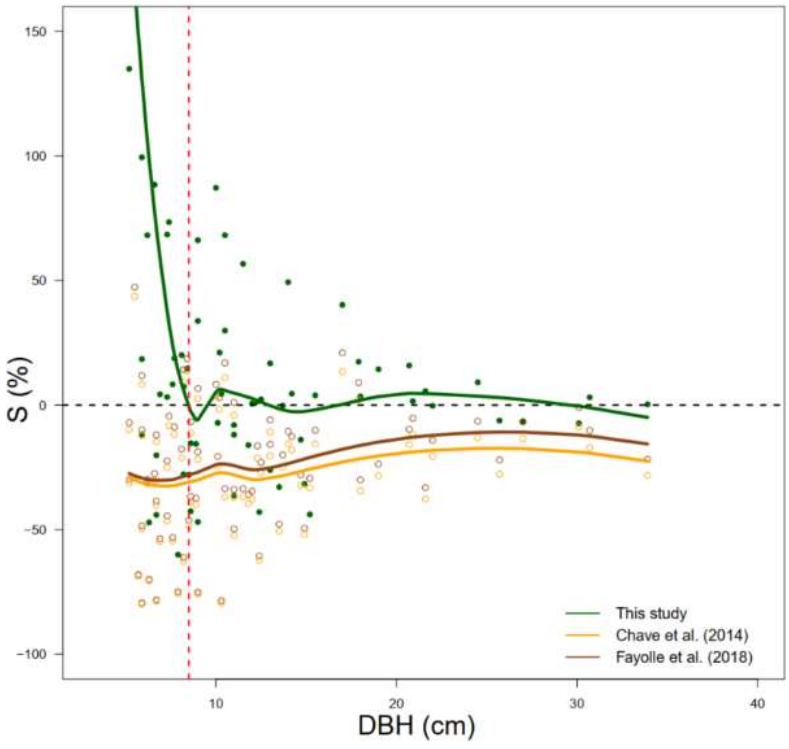

Figure 5. Size-dependent deviations in AGB predictions, relative error (S, in %) across DBH classes for MLS-derived and allometric estimates.

4. Discussion

4.1. Foliar Biomass to Tropical AGB and Implications for Forest Structure

Our results demonstrate that foliar biomass constitutes for a small fraction of total aboveground biomass (AGB), around 3% on average across species and diameter classes. Although this proportion is modest compared to woody compartments, it is fully consistent with previous destructive studies

 doi:10.20944/preprints202603.1717.v1

reporting leaf contributions ranging between 2% and 15% depending on species and forest type (Kenzo et al., 2010; Kossi Ditsouga et al., 2024; Salis et al., 2006). Importantly, we also show that leaf allocation decreases with tree size, with young individuals (<10 cm DBH) exhibiting higher proportional investment in crown structures. This ontogenetic shift aligns with established ecological theory, which describes that small trees prioritize crown expansion for light interception, whereas larger trees allocate more resources to stem thickening and mechanical stability (Jucker et al., 2017; Poorter et al., 2015). The similarity in biomass partitioning between shade-tolerant (NPLD) and pioneer (P) species was particularly notable. Despite differences in known successional strategies, both guilds exhibited highly comparable proportional investment across compartments. This suggests that both regenerating or plantation forests may impose similar constraints on trees, leading to convergent biomass allocation patterns, as has been reported for other disturbed tropical systems (Banin et al., 2012; Feldpausch et al., 2012; Gourlet-Fleury et al., 2011).

4.2. Performance of LiDAR-Derived Models for Predicting Foliar Mass

Considering crown-based LiDAR metrics significantly improved the prediction of total leaf mass (TLM). While DBH alone explained a substantial portion of the variance (48%), adding projected crown area (PCA) increased predictive performance and reduced uncertainty. These findings reinforce the idea that crown geometry rather than stem size alone captures key functional and structural determinants of leaf biomass (Jucker et al., 2022; Lines et al., 2022). The additional improvement achieved by including wood density (WD) highlights the importance of integrating species-specific functional traits into LiDAR-based biomass models (Jensen, 2025). Cross-validation confirmed the robustness of our models across hierarchical levels. RMSE values were narrow and highly consistent between individual and species-level validation, indicating limited overfitting and it potential for generalization. Few tropical studies have performed such rigorous validation on destructively sampled datasets, which strengthens the reliability of our approach (Gonzalez de Tanago et al., 2017; Goodman et al., 2014; Lau et al., 2019a). Together, these results demonstrate that mobile LiDAR scanning (MLS) can yield precise, repeatable estimations of leaf biomass even in structurally complex understories.

A key outcome of this study is that combining MLS-derived woody volume with an explicit leaf-mass term yields AGB estimates that closely match destructive measurements. MLS-based AGB using woody biomass alone was already very close to observations (bias ≈ -2%), and adding model-predicted TLM further reduced this small residual bias (to +1.9%). This change builds on the fact that tree volumes are directly computed from detailed MLS geometry, rather than inferred from generic allometric coefficients. A choice that largely explains the discrepancy with the regional equation, which clearly underestimates AGB in these plantations. Importantly, most existing TLS/MLS-based AGB studies still ignore foliage, assuming its contribution to be negligible (Calders et al., 2015; Gonzalez de Tanago et al., 2018, 2017; Lau et al., 2019b; Momo Takoudjou et al., 2018). If foliar biomass were genuinely negligible for carbon accounting, it would be difficult to rationalize the considerable effort invested over the last five years in leaf–wood segmentation, or the proliferation of algorithms and software expressly designed to disentangle foliage from woody elements in LiDAR point clouds (Jiang et al., 2023; Tian and Li, 2022; Wang et al., 2020; Wilkes et al., 2023). Our results confirm that although leaf mass is small, its omission introduces systematic underestimation especially in young stands, regenerating forests, and small-diameter classes. These improvements are particularly evident when MLS estimates are compared to classic allometries. Both the regional model of Fayolle et al. (2018) and the pantropical model of Chave et al. ,(2014) exhibited strong negative bias (-20% to -26%), in line with accumulating evidence that allometries often underpredict biomass in dense or structurally complex tropical forests (Blanchard et al., 2016; Demol et al., 2022; Ploton et al., 2016). Our results show that MLS with foliar integration not only reduces these biases but also aligns far more closely with observed AGB across size classes.

4.3. DBH-Dependent Errors

 doi:10.20944/preprints202603.1717.v1

Size-dependent error analysis revealed critical performance differences between MLS-based and allometric predictions. For small trees (<8 cm DBH), MLS tended to overestimate AGB while allometries strongly underestimated it. Such divergence reflects two structural limitations: i) allometries are poorly calibrated for small trees, as they largely rely on datasets dominated by mid to large sized individuals (Chave et al., 2014; Fayolle et al., 2018); ii) MLS accurately captures crown architecture, which is disproportionately important in small trees, whereas allometries rely primarily on DBH a weak predictor of aboveground structure at early growth stages. For intermediate trees, MLS predictions were nearly unbiased (S ≈ 0%), while allometries maintained their systematic underestimation. This is consistent with the idea that LiDAR provides direct structural information, crown volume, branch topology that allometries can only approximate (Disney, 2019; Malhi et al., 2018; Matheus Boni Vicari et al., 2019). In larger trees, error levels converged but MLS estimates remained consistently closer to zero, suggesting that LiDAR maintains accuracy even when stem geometry becomes more complex and crown morphology asymmetric (Blanchard et al., 2016; Ploton et al., 2016). This has major implications for carbon accounting, forest restoration monitoring, and REDD+ programs, which critically depend on accurate AGB estimation (Chave et al., 2019; Duncanson et al., 2021; Réjou-Méchain et al., 2019; Schepaschenko et al., 2019). Beyond improving model fit, our results show that foliar biomass varies significantly among species and across size classes, rather than representing a constant fraction of AGB. This interspecific variability likely reflects contrasting functional and architectural strategies, with implications for LiDAR-based biomass models that assume uniform allocation rules. By explicitly linking three-dimensional crown structure to leaf mass, our study shows that foliage sits at the interface between fine-scale canopy architecture, key ecological functions such as light interception and carbon assimilation, and robust estimation of AGB. In this sense, integrating leaves into LiDAR workflows is not a marginal correction, but a shift in perspective that more tightly connects structure, function and carbon.

Conclusion

Our study demonstrates that explicitly accounting for leaf biomass can improve the accuracy of aboveground biomass (AGB) predictions derived from LiDAR scanning in tropical forests. Beyond improving tree-level estimates, our results reveal size-dependent deviations that explain long-standing discrepancies observed with pantropical and regional allometries. LiDAR derived AGB was nearly unbiased across most of the diameter range, whereas classical allometries exhibited persistent negative errors linked to their inability to characterize crown structure and species-specific allocation strategies. These findings reinforce the idea that canopy architecture, rather than DBH alone, is a critical driver of biomass variability particularly in regenerating or forests. By providing the first empirical evidence that leaf mass can be reliably predicted from 3D crown traits and meaningfully incorporated into non-destructive biomass assessments, this study bridges a key gap between destructive and LiDAR-based approaches. It supports the integration of LiDAR into monitoring programs for restoration forests and carbon accounting. Future research should explore scaling these methods to stand and landscape levels, integrating temporal dynamics, and combining MLS with UAV or satellite LiDAR to refine pantropical carbon maps.

Author Contributions: Conceptualization S.T.M., P.A.M.M.Z. and A.B.; formal analysis, S.T.M; investigation, S.T.M P.A.M.M.Z., ST. and A.B.; data curation, S.T.M., P.A.M.M.Z., H.K., Y.S.N., and A.B. writing original draft, S.T.M., A.B., BS. and J.L.D. All authors have read and agreed to the published version of the manuscript.

Data Availability Statement: Requests for data and materials should be addressed to the first author at takoudjoumomo@gmail.com.

Acknowledgments: This research was made possible with the support of the Applied Research in Ecology and Social Sciences in Support of the Sustainable Management of Forest Ecosystems in Central Africa (RESSAC) program implemented by CIFOR-ICRAF, and with the financial assistance of the European Union. We are also

 doi:10.20944/preprints202603.1717.v1

grateful to Philippe Lejeune, Jean-Yves De Vleeschouwer, direction and staff of Pallisco company, especially Richard Fétéke and all their support during field missions.

Conflicts of Interest: The authors declare no conflicts of interest.

References

Åkerblom, M., Raumonen, P., Mäkipää, R., Kaasalainen, M., 2017. Automatic tree species recognition with quantitative structure models. Remote Sens. Environ. 191, 1–12. https://doi.org/10.1016/j.rse.2016.12.002

Banin, L., Feldpausch, T.R., Phillips, O.L., Baker, T.R., Lloyd, J., Affum-Baffoe, K., Arets, E.J.M.M., Berry, N.J., Bradford, M., Brienen, R.J.W., Davies, S., Drescher, M., Higuchi, N., Hilbert, D.W., Hladik, A., Iida, Y., Salim, K.A., Kassim, A.R., King, D.A., Lopez-Gonzalez, G., Metcalfe, D., Nilus, R., Peh, K.S.H., Reitsma, J.M., Sonké, B., Taedoumg, H., Tan, S., White, L., Wöll, H., Lewis, S.L., 2012. What controls tropical forest architecture? Testing environmental, structural and floristic drivers. Global Ecology and Biogeography 21, 1179–1190. https://doi.org/10.1111/j.1466-8238.2012.00778.x

Bastin, J.-F., Rutishauser, E., Kellner, J.R., Saatchi, S., Pélissier, R., Hérault, B., Slik, F., Bogaert, J., De Cannière, C., Marshall, A.R., Poulsen, J., Alvarez-Loyayza, P., Andrade, A., Angbonga-Basia, A., Araujo-Murakami, A., Arroyo, L., Ayyappan, N., de Azevedo, C.P., Banki, O., Barbier, N., Barroso, J.G., Beeckman, H., Bitariho, R., Boeckx, P., Boehning-Gaese, K., Brandão, H., Brearley, F.Q., Breuer Ndoundou Hockemba, M., Brienen, R., Camargo, J.L.C., Campos-Arceiz, A., Cassart, B., Chave, J., Chazdon, R., Chuyong, G., Clark, D.B., Clark, C.J., Condit, R., Honorio Coronado, E.N., Davidar, P., de Haulleville, T., Descroix, L., Doucet, J.-L., Dourdain, A., Droissart, V., Duncan, T., Silva Espejo, J., Espinosa, S., Farwig, N., Fayolle, A., Feldpausch, T.R., Ferraz, A., Fletcher, C., Gajapersad, K., Gillet, J.-F., Amaral, I.L. do, Gonmadje, C., Grogan, J., Harris, D., Herzog, S.K., Homeier, J., Hubau, W., Hubbell, S.P., Hufkens, K., Hurtado, J., Kamdem, N.G., Kearsley, E., Kenfack, D., Kessler, M., Labrière, N., Laumonier, Y., Laurance, S., Laurance, W.F., Lewis, S.L., Libalah, M.B., Ligot, G., Lloyd, J., Lovejoy, T.E., Malhi, Y., Marimon, B.S., Marimon Junior, B.H., Martin, E.H., Matius, P., Meyer, V., Mendoza Bautista, C., Monteagudo-Mendoza, A., Mtui, A., Neill, D., Parada Gutierrez, G.A., Pardo, G., Parren, M., Parthasarathy, N., Phillips, O.L., Pitman, N.C.A., Ploton, P., Ponette, Q., Ramesh, B.R., Razafimahaimodison, J.-C., Réjou-Méchain, M., Rolim, S.G., Saltos, H.R., Rossi, L.M.B., Spironello, W.R., Rovero, F., Saner, P., Sasaki, D., Schulze, M., Silveira, M., Singh, J., Sist, P., Sonke, B., Soto, J.D., de Souza, C.R., Stropp, J., Sullivan, M.J.P., Swanepoel, B., Steege, H. ter, Terborgh, J., Texier, N., Toma, T., Valencia, R., Valenzuela, L., Ferreira, L.V., Valverde, F.C., Van Andel, T.R., Vasque, R., Verbeeck, H., Vivek, P., Vleminckx, J., Vos, V.A., Wagner, F.H., Warsudi, P.P., Wortel, V., Zagt, R.J., Zebaze, D., 2018. Pan-tropical prediction of forest structure from the largest trees. Global Ecology and Biogeography 1–18. https://doi.org/10.1111/geb.12803

Bauwens, S., Bartholomeus, H., Calders, K., Lejeune, P., 2016. Forest inventory with terrestrial LiDAR: A comparison of static and hand-held mobile laser scanning. Forests 7, 127. https://doi.org/10.3390/f7060127

Blanchard, E., Birnbaum, P., Ibanez, T., Boutreux, T., Antin, C., Ploton, P., Vincent, G., Pouteau, R., Vandrot, H., Hequet, V., Barbier, N., Droissart, V., Sonké, B., Texier, N., Kamdem, N.G., Zebaze, D., Libalah, M., Couteron, P., 2016. Contrasted allometries between stem diameter, crown area, and tree height in five tropical biogeographic areas. Trees - Structure and Function 30, 1953–1968. https://doi.org/10.1007/S00468-016-1424-3

Bonan, G.B., 2008. Forests and climate change: Forcings, feedbacks, and the climate benefits of forests. Science (1979). 320, 1444–1449. https://doi.org/10.1126/science.1155121

Brown, S., Gillespie, A.J.R., Lugo, A.E., 1989. Estimation methods for tropical forests.pdf.

Burt, A., Boni Vicari, M., Da Costa, A.C.L., Coughlin, I., Meir, P., Rowland, L., Disney, M., 2021. New insights into large tropical tree mass and structure from direct harvest and terrestrial lidar. R. Soc. Open Sci. 8. https://doi.org/10.1098/rsos.201458

Burt, A., Disney, M., Calders, K., 2019. Extracting individual trees from lidar point clouds using treeseg. Methods Ecol. Evol. 10, 438–445. https://doi.org/10.1111/2041-210X.13121

 doi:10.20944/preprints202603.1717.v1

Calders, K., Newnham, G., Burt, A., Murphy, S., Raumonen, P., Herold, M., Culvenor, D., Avitabile, V., Disney, M., Armston, J., Kaasalainen, M., 2015. Nondestructive estimates of above-ground biomass using terrestrial laser scanning. Methods Ecol. Evol. 6, 198–208. https://doi.org/10.1111/2041-210X.12301

Chave, J., 2005. Tree height measurement protocol – J Chave Measuring tree height for tropical forest trees A field manual for the CTFS sites.

Chave, J., Andalo, C., Brown, S., Cairns, M.A., Chambers, J.Q., Eamus, D., Fölster, H., Fromard, F., Higuchi, N., Kira, T., Lescure, J.-P., Nelson, B.W., Ogawa, H., Puig, H., Riéra, B., Yamakura, T., 2005. Tree allometry and improved estimation of carbon stocks and balance in tropical forests. Oecologia 145, 87–99. https://doi.org/10.1007/s00442-005-0100-x

Chave, J., Davies, S.J., Phillips, O.L., Lewis, S.L., Sist, P., Schepaschenko, D., Armston, J., Baker, T.R., Coomes, D., Disney, M., Duncanson, L., Hérault, B., Labrière, N., Meyer, V., Réjou-Méchain, M., Scipal, K., Saatchi, S., 2019. Ground Data are Essential for Biomass Remote Sensing Missions. Surv. Geophys. https://doi.org/10.1007/s10712-019-09528-w

Chave, J., Réjou-Méchain, M., Búrquez, A., Chidumayo, E., Colgan, M.S., Delitti, W.B.C., Duque, A., Eid, T., Fearnside, P.M., Goodman, R.C., Henry, M., Martínez-Yrízar, A., Mugasha, W.A., Muller-Landau, H.C., Mencuccini, M., Nelson, B.W., Ngomanda, A., Nogueira, E.M., Ortiz-Malavassi, E., Pélissier, R., Ploton, P., Ryan, C.M., Saldarriaga, J.G., Vieilledent, G., 2014. Improved allometric models to estimate the aboveground biomass of tropical trees. Glob. Chang. Biol. 20, 3177–3190. https://doi.org/10.1111/gcb.12629

Demol, M., Calders, K., Krishna Moorthy, S.M., Van den Bulcke, J., Verbeeck, H., Gielen, B., 2021. Consequences of vertical basic wood density variation on the estimation of aboveground biomass with terrestrial laser scanning. Trees - Structure and Function 35, 671–684. https://doi.org/10.1007/s00468-020-02067-7

Demol, M., Verbeeck, H., Gielen, B., Armston, J., Burt, A., Disney, M., Duncanson, L., Hackenberg, J., Kükenbrink, D., Lau, A., Ploton, P., Sewdien, A., Stovall, A., Takoudjou, S.M., Volkova, L., Weston, C., Wortel, V., Calders, K., 2022. Estimating forest above-ground biomass with terrestrial laser scanning: Current status and future directions. Methods Ecol. Evol. 13, 1628–1639. https://doi.org/10.1111/2041-210X.13906

Díaz, S., Kattge, J., Cornelissen, J.H.C., Wright, I.J., Lavorel, S., Dray, S., Reu, B., Kleyer, M., Wirth, C., Colin Prentice, I., Garnier, E., Bönisch, G., Westoby, M., Poorter, H., Reich, P.B., Moles, A.T., Dickie, J., Gillison, A.N., Zanne, A.E., Chave, J., Joseph Wright, S., Sheremet Ev, S.N., Jactel, H., Baraloto, C., Cerabolini, B., Pierce, S., Shipley, B., Kirkup, D., Casanoves, F., Joswig, J.S., Günther, A., Falczuk, V., Rüger, N., Mahecha, M.D., Gorné, L.D., 2016. The global spectrum of plant form and function. Nature 529, 167–171. https://doi.org/10.1038/nature16489

Disney, M., 2019. Terrestrial LiDAR: a three-dimensional revolution in how we look at trees. New Phytologist 222, 1736–1741. https://doi.org/10.1111/NPH.15517

Disney, M., Burt, A., Calders, K., Schaaf, C., Stovall, A., 2019. Innovations in Ground and Airborne Technologies as Reference and for Training and Validation: Terrestrial Laser Scanning (TLS). Surv. Geophys. 40, 937–958. https://doi.org/10.1007/s10712-019-09527-x

Disney, M.I., Boni Vicari, M., Burt, A., Calders, K., Lewis, S.L., Raumonen, P., Wilkes, P., 2018. Weighing trees with lasers: Advances, challenges and opportunities. Interface Focus 8. https://doi.org/10.1098/rsfs.2017.0048

Djomo, A.N., Chimi, C.D., 2017. Tree allometric equations for estimation of above, below and total biomass in a tropical moist forest: Case study with application to remote sensing. For. Ecol. Manage. 391, 184–193. https://doi.org/10.1016/j.foreco.2017.02.022

Djomo, A.N., Ibrahima, A., Saborowski, J., Gravenhorst, G., 2010. Allometric equations for biomass estimations in Cameroon and pan moist tropical equations including biomass data from Africa. For. Ecol. Manage. 260, 1873–1885. https://doi.org/10.1016/j.foreco.2010.08.034

Dorisca, S., Durrieur, M.D.L., Fontez, B., Giraud, A., Riera, B., 2011. Équations Entre Le Diamètre Et Le Volume Total. Bois et Forêts des Tropiques 308, 87–95.

Doucet, J.L., Daïnou, K., Ligot, G., Ouédraogo, D.Y., Bourland, N., Ward, S.E., Tekam, P., Lagoute, P., Fayolle, A., 2016. Enrichment of Central African logged forests with high-value tree species: testing a new approach

 doi:10.20944/preprints202603.1717.v1

to regenerating degraded forests. Int. J. Biodivers. Sci. Ecosyst. Serv. Manag. 12, 83–95. https://doi.org/10.1080/21513732.2016.1168868

Droissart, V., Verlynde, S., Ramandimbisoa, B., Andriamahefarivo, L., Stévart, T., 2023. Diversity and distribution of Orchidaceae in one of the world's most threatened plant hotspots (Madagascar). Biodivers. Data J. 11, e106223. https://doi.org/10.3897/BDJ.11.E106223

Duncanson, L., Disney, M., Armston, J., Nickeson, J., Minor, D., 2021. Committee on Earth Observation Satellites Working Group on Calibration and Validation Land Product Validation Subgroup Aboveground Woody Biomass Product Validation Good Practices Protocol. Good Practices for Satellite Derived Land Product Validation 0–236. https://doi.org/10.5067/doc/ceoswgcv/lpv/agb.001

Fayolle, A., Doucet, J.L., Gillet, J.F., Bourland, N., Lejeune, P., 2013. Tree allometry in Central Africa: Testing the validity of pantropical multi-species allometric equations for estimating biomass and carbon stocks. For. Ecol. Manage. 305, 29–37. https://doi.org/10.1016/j.foreco.2013.05.036

Fayolle, A., Ngomanda, A., Mbasi, M., Barbier, N., Bocko, Y., Boyemba, F., Couteron, P., Fonton, N., Kamdem, N., Katembo, J., Kondaoule, H.J., Loumeto, J., Maïdou, H.M., Mankou, G., Mengui, T., Mofack, G.I., Moundounga, C., Moundounga, Q., Nguimbous, L., Nsue Nchama, N., Obiang, D., Ondo Meye Asue, F., Picard, N., Rossi, V., Senguela, Y.P., Sonké, B., Viard, L., Yongo, O.D., Zapfack, L., Medjibe, V.P., 2018. A regional allometry for the Congo basin forests based on the largest ever destructive sampling. For. Ecol. Manage. 430, 228–240. https://doi.org/10.1016/j.foreco.2018.07.030

Feldpausch, T.R., Lloyd, J., Lewis, S.L., Brienen, R.J.W., Gloor, M., Monteagudo Mendoza, A., Lopez-Gonzalez, G., Banin, L., Abu Salim, K., Affum-Baffoe, K., Alexiades, M., Almeida, S., Amaral, I., Andrade, A., Aragão, L.E.O.C., Araujo Murakami, A., Arets, E.J.M., Arroyo, L., Aymard C., G.A., Baker, T.R., Bánki, O.S., Berry, N.J., Cardozo, N., Chave, J., Comiskey, J.A., Alvarez, E., De Oliveira, A., Di Fiore, A., Djagbletey, G., Domingues, T.F., Erwin, T.L., Fearnside, P.M., França, M.B., Freitas, M.A., Higuchi, N., Honorio C., E., Iida, Y., Jiménez, E., Kassim, A.R., Killeen, T.J., Laurance, W.F., Lovett, J.C., Malhi, Y., Marimon, B.S., Marimon-Junior, B.H., Lenza, E., Marshall, A.R., Mendoza, C., Metcalfe, D.J., Mitchard, E.T.A., Neill, D.A., Nelson, B.W., Nilus, R., Nogueira, E.M., Parada, A., S.-H. Peh, K., Pena Cruz, A., Peñuela, M.C., Pitman, N.C.A., Prieto, A., Quesada, C.A., Ramírez, F., Ramírez-Angulo, H., Reitsma, J.M., Rudas, A., Saiz, G., Salomão, R.P., Schwarz, M., Silva, N., Silva-Espejo, J.E., Silveira, M., Sonké, B., Stropp, J., Taedoumg, H.E., Tan, S., Ter Steege, H., Terborgh, J., Torello-Raventos, M., Van Der Heijden, G.M.F., Vásquez, R., Vilanova, E., Vos, V.A., White, L., Willcock, S., Woell, H., Phillips, O.L., 2012. Tree height integrated into pantropical forest biomass estimates. Biogeosciences 9, 3381–3403. https://doi.org/10.5194/bg-9-3381-2012

Gonzalez de Tanago, J., Lau, A., Bartholomeus, H., Herold, M., Avitabile, V., Raumonen, P., Martius, C., Goodman, R.C., Disney, M., Manuri, S., Burt, A., Calders, K., 2018. Estimation of above-ground biomass of large tropical trees with terrestrial LiDAR. Methods Ecol. Evol. 9, 223–234. https://doi.org/10.1111/2041-210X.12904

Gonzalez de Tanago, J.M., Lau, A., Bartholomeusm, H., Herold, M., Valerio, A., Raumonen, P., Martius, C., Goodman, R., Disney, M., Manuri, S., Burt, A., Calders, K., 2017. Estimation of above -ground biomass of large tropical trees with Terrestrial LiDARof results obtained in the DULCIS study. https://doi.org/DOI: 10.1111/2041-210X.12904

Goodman, R.C., Phillips, O.L., Baker, T.R., 2014. The importance of crown dimensions to improve tropical tree biomass estimates. Ecological Applications 24, 680–698. https://doi.org/10.1890/13-0070.1

Gourlet-Fleury, S., Rossi, V., Rejou-Mechain, M., Freycon, V., Fayolle, A., Saint-André, L., Cornu, G., Gérard, J., Sarrailh, J.M., Flores, O., Baya, F., Billand, A., Fauvet, N., Gally, M., Henry, M., Hubert, D., Pasquier, A., Picard, N., 2011. Environmental filtering of dense-wooded species controls above-ground biomass stored in African moist forests. Journal of Ecology 99, 981–990. https://doi.org/10.1111/j.1365-2745.2011.01829.x

Hackenberg, J., Morhart, C., Sheppard, J., Spiecker, H., Disney, M., 2014. Highly accurate tree models derived from terrestrial laser scan data: A method description. Forests 5, 1069–1105. https://doi.org/10.3390/f5051069

Hackenberg, J., Spiecker, H., Calders, K., Disney, M., Raumonen, P., 2015a. SimpleTree - An efficient open source tool to build tree models from TLS clouds. Forests 6, 4245–4294. https://doi.org/10.3390/f6114245

 doi:10.20944/preprints202603.1717.v1

Hackenberg, J., Wassenberg, M., Spiecker, H., Sun, D., 2015b. Non destructive method for biomass prediction combining TLS derived tree volume and wood density. Forests 6, 1274–1300. https://doi.org/10.3390/f6041274

Hallé, Francis., Oldeman, R.A.A., Tomlinson, P.B., 1978. Tropical Trees and Forests : an Architectural Analysis. Springer Berlin Heidelberg.

Hubau, W., Lewis, S.L., Phillips, O.L., Affum-Baffoe, K., Beeckman, H., Cuní-Sanchez, A., Daniels, A.K., Ewango, C.E.N., Fauset, S., Mukinzi, J.M., Sheil, D., Sonké, B., Sullivan, M.J.P., Sunderland, T.C.H., Taedoumg, H., Thomas, S.C., White, L.J.T., Abernethy, K.A., Adu-Bredu, S., Amani, C.A., Baker, T.R., Banin, L.F., Baya, F., Begne, S.K., Bennett, A.C., Benedet, F., Bitariho, R., Bocko, Y.E., Boeckx, P., Boundja, P., Brienen, R.J.W., Brncic, T., Chezeaux, E., Chuyong, G.B., Clark, C.J., Collins, M., Comiskey, J.A., Coomes, D.A., Dargie, G.C., de Haulleville, T., Kamdem, M.N.D., Doucet, J.L., Esquivel-Muelbert, A., Feldpausch, T.R., Fofanah, A., Foli, E.G., Gilpin, M., Gloor, E., Gonmadje, C., Gourlet-Fleury, S., Hall, J.S., Hamilton, A.C., Harris, D.J., Hart, T.B., Hockemba, M.B.N., Hladik, A., Ifo, S.A., Jeffery, K.J., Jucker, T., Yakusu, E.K., Kearsley, E., Kenfack, D., Koch, A., Leal, M.E., Levesley, A., Lindsell, J.A., Lisingo, J., Lopez-Gonzalez, G., Lovett, J.C., Makana, J.R., Malhi, Y., Marshall, A.R., Martin, J., Martin, E.H., Mbayu, F.M., Medjibe, V.P., Mihindou, V., Mitchard, E.T.A., Moore, S., Munishi, P.K.T., Bengone, N.N., Ojo, L., Ondo, F.E., Peh, K.S.H., Pickavance, G.C., Poulsen, A.D., Poulsen, J.R., Qie, L., Reitsma, J., Rovero, F., Swaine, M.D., Talbot, J., Taplin, J., Taylor, D.M., Thomas, D.W., Toirambe, B., Mukendi, J.T., Tuagben, D., Umunay, P.M., van der Heijden, G.M.F., Verbeeck, H., Vleminckx, J., Willcock, S., Wöll, H., Woods, J.T., Zemagho, L., 2020. Asynchronous carbon sink saturation in African and Amazonian tropical forests. Nature 579, 80–87. https://doi.org/10.1038/s41586-020-2035-0

Jackson, T., Shenkin, A., Moore, J., Bunce, A., Van Emmerik, T., Kane, B., Burcham, D., James, K., Selker, J., Calders, K., Origo, N., Disney, M., Burt, A., Wilkes, P., Raumonen, P., Gonzalez De Tanago Menaca, J., Lau, A., Herold, M., Goodman, R.C., Fourcaud, T., Malhi, Y., 2019. An architectural understanding of natural sway frequencies in trees. J. R. Soc. Interface 16. https://doi.org/10.1098/rsif.2019.0116

Jensen, J., 2025. Linking tree species diversity , productivity , and carbon sequestration in mixed-species forest plantations From patterns to mechanisms Linking tree species diversity , productivity , and carbon sequestration. SWEDISH UNIVERSITY OF AGRICULTURAL SCIENCES : SLU.

Jiang, T., Zhang, Q., Liu, S., Liang, C., Dai, L., Zhang, Z., Sun, J., Wang, Y., 2023. LWSNet: A Point-Based Segmentation Network for Leaf-Wood Separation of Individual Trees. Forests 14. https://doi.org/10.3390/f14071303

Jones, A., Breuning-Madsen, H., Brossard, M., Dampha, A., Deckers, J., Dewitte, O., Kilasara, M., 2013. Soil atlas of Africa (Luxembourg: European Commission, Publications Office of the European Union).

Jucker, T., Caspersen, J., Chave, J., Antin, C., Barbier, N., Bongers, F., Dalponte, M., van Ewijk, K.Y., Forrester, D.I., Haeni, M., Higgins, S.I., Holdaway, R.J., Iida, Y., Lorimer, C., Marshall, P.L., Momo, S., Moncrieff, G.R., Ploton, P., Poorter, L., Rahman, K.A., Schlund, M., Sonké, B., Sterck, F.J., Trugman, A.T., Usoltsev, V.A., Vanderwel, M.C., Waldner, P., Wedeux, B.M.M., Wirth, C., Wöll, H., Woods, M., Xiang, W., Zimmermann, N.E., Coomes, D.A., 2017. Allometric equations for integrating remote sensing imagery into forest monitoring programmes. Glob. Chang. Biol. 23, 177–190. https://doi.org/10.1111/gcb.13388

Jucker, T., Fischer, F.J., Chave, J., Coomes, D.A., Caspersen, J., Ali, A., Loubota Panzou, G.J., Feldpausch, T.R., Falster, D., Usoltsev, V.A., Adu-Bredu, S., Alves, L.F., Aminpour, M., Angoboy, I.B., Anten, N.P.R., Antin, C., Askari, Y., Muñoz, R., Ayyappan, N., Balvanera, P., Banin, L., Barbier, N., Battles, J.J., Beeckman, H., Bocko, Y.E., Bond-Lamberty, B., Bongers, F., Bowers, S., Brade, T., van Breugel, M., Chantrain, A., Chaudhary, R., Dai, J., Dalponte, M., Dimobe, K., Domec, J.C., Doucet, J.L., Duursma, R.A., Enríquez, M., van Ewijk, K.Y., Farfán-Rios, W., Fayolle, A., Forni, E., Forrester, D.I., Gilani, H., Godlee, J.L., Gourlet-Fleury, S., Haeni, M., Hall, J.S., He, J.K., Hemp, A., Hernández-Stefanoni, J.L., Higgins, S.I., Holdaway, R.J., Hussain, K., Hutley, L.B., Ichie, T., Iida, Y., Jiang, H. sheng, Joshi, P.R., Kaboli, H., Larsary, M.K., Kenzo, T., Kloeppel, B.D., Kohyama, T., Kunwar, S., Kuyah, S., Kvasnica, J., Lin, S., Lines, E.R., Liu, H., Lorimer, C., Loumeto, J.J., Malhi, Y., Marshall, P.L., Mattsson, E., Matula, R., Meave, J.A., Mensah, S., Mi, X., Momo, S., Moncrieff, G.R., Mora, F., Nissanka, S.P., O'Hara, K.L., Pearce, S., Pelissier, R., Peri, P.L., Ploton, P., Poorter, L., Pour, M.J., Pourbabaei, H., Dupuy-Rada, J.M., Ribeiro, S.C., Ryan, C., Sanaei, A., Sanger, J.,

 doi:10.20944/preprints202603.1717.v1

Schlund, M., Sellan, G., Shenkin, A., Sonké, B., Sterck, F.J., Svátek, M., Takagi, K., Trugman, A.T., Ullah, F., Vadeboncoeur, M.A., Valipour, A., Vanderwel, M.C., Vovides, A.G., Wang, W., Wang, L.Q., Wirth, C., Woods, M., Xiang, W., Ximenes, F. de A., Xu, Y., Yamada, T., Zavala, M.A., 2022. Tallo: A global tree allometry and crown architecture database. Glob. Chang. Biol. 28, 5254–5268. https://doi.org/10.1111/gcb.16302

Jucker, T., Fischer, F.J., Chave, J., Coomes, D.A., Caspersen, J., Ali, A., Loubota Panzou, G.J., Feldpausch, T.R., Falster, D., Usoltsev, V.A., Jackson, T.D., Adu-Bredu, S., Alves, L.F., Aminpour, M., Angoboy Ilondea, B., Anten, N.P.R., Antin, C., Askari, Y., Ayyappan, N., Banin, L.F., Barbier, N., Battles, J.J., Beeckman, H., Bocko, Y.E., Bond-Lamberty, B., Bongers, F., Bowers, S., van Breugel, M., Chantrain, A., Chaudhary, R., Dai, J., Dalponte, M., Dimobe, K., Domec, J.C., Doucet, J.L., Dupuy Rada, J.M., Duursma, R.A., Enríquez, M., van Ewijk, K.Y., Farfán-Rios, W., Fayolle, A., Ferretti, M., Forni, E., Forrester, D.I., Gilani, H., Godlee, J.L., Haeni, M., Hall, J.S., He, J.K., Hemp, A., Hernández-Stefanoni, J.L., Higgins, S.I., Holdaway, R.J., Hussain, K., Hutley, L.B., Ichie, T., Iida, Y., Jiang, H.S., Joshi, P.R., Kaboli, H., Kazempour Larsary, M., Kenzo, T., Kloeppel, B.D., Kohyama, T.S., Kunwar, S., Kuyah, S., Kvasnica, J., Lin, S., Lines, E.R., Liu, H., Lorimer, C., Loumeto, J.J., Malhi, Y., Marshall, P.L., Mattsson, E., Matula, R., Meave, J.A., Mensah, S., Mi, X., Momo, S.T., Moncrieff, G.R., Mora, F., Muñoz, R., Nissanka, S.P., Nur Hajar, Z.S., O'Hara, K.L., Pearce, S., Pelissier, R., Peri, P.L., Ploton, P., Poorter, L., Pour, M.J., Pourbabaei, H., Ribeiro, S.C., Ryan, C., Sanaei, A., Sanger, J., Schlund, M., Sellan, G., Shenkin, A., Sonké, B., Sterck, F.J., Svátek, M., Takagi, K., Trugman, A.T., Vadeboncoeur, M.A., Valipour, A., Vanderwel, M.C., Vovides, A.G., Waldner, P., Wang, W., Wang, L.Q., Wirth, C., Woods, M., Xiang, W., de Aquino Ximenes, F., Xu, Y., Yamada, T., Zavala, M.A., Zimmermann, N.E., 2025. The global spectrum of tree crown architecture. Nature Communications 16, 45–50. https://doi.org/10.1038/s41467-025-60262-x

Kaasalainen, S., Krooks, A., Liski, J., Raumonen, P., Kaartinen, H., Kaasalainen, M., Puttonen, E., Anttila, K., Mäkipää, R., Kaasalainen, S., Krooks, A., Liski, J., Raumonen, P., Kaartinen, H., Kaasalainen, M., Puttonen, E., Anttila, K., Mäkipää, R., 2014. Change Detection of Tree Biomass with Terrestrial Laser Scanning and Quantitative Structure Modelling. Remote Sens. (Basel). 6, 3906–3922. https://doi.org/10.3390/rs6053906

Kenzo, T., Ichie, T., Hattori, D., Kendawang, J.J., Sakurai, K., Ninomiya, I., 2010. Changes in above- and belowground biomass in early successional tropical secondary forests after shifting cultivation in Sarawak, Malaysia. For. Ecol. Manage. 260, 875–882. https://doi.org/10.1016/j.foreco.2010.06.006

Kossi Ditsouga, A.F., Moundounga Mavouroulou, Q., Moundounga, C.G., Fayolle, A., Picard, N., Sato, A., Ngomanda, A., 2024. Tree belowground biomass in Congo Basin forests: allometric equations and scaling with aboveground biomass. Forestry: An International Journal of Forest Research 1–10. https://doi.org/10.1093/forestry/cpae009

Lau, A., Calders, K., Bartholomeus, H., Martius, C., Raumonen, P., Herold, M., Vicari, M., Sukhdeo, H., Singh, J., Goodman, R.C., 2019a. Tree biomass equations from terrestrial LiDAR: A case study in Guyana. Forests 10, 1–18. https://doi.org/10.3390/f10060527

Lau, A., Martius, C., Bartholomeus, H., Shenkin, A., Jackson, T., Malhi, Y., Herold, M., Bentley, L.P., 2019b. Estimating architecture-based metabolic scaling exponents of tropical trees using terrestrial LiDAR and 3D modelling. For. Ecol. Manage. 439, 132–145. https://doi.org/10.1016/j.foreco.2019.02.019

Letouzey, R., 1985. Carte phytogéographique du Cameroun, 1:500 000, 8 feuillets + 5 notices. Toulouse, France.

Lines, E.R., Fischer, F.J., Owen, H.J.F., Jucker, T., 2022. The shape of trees: reimagining forest ecology in three dimensions with remote sensing. Journal of Ecology 1–16. https://doi.org/10.1111/1365-2745.13944

Malhi, Y., Jackson, T., Bentley, L.P., Lau, A., Shenkin, A., Herold, M., Calders, K., Bartholomeus, H., Disney, M.I., 2018. New perspectives on the ecology of tree structure and tree communities through terrestrial laser scanning. Interface Focus 8, 2015–2017. https://doi.org/10.1098/rsfs.2017.0052

Martin-Ducup, O., Mofack, G., Wang, D., Raumonen, P., Ploton, P., Sonké, B., Barbier, N., Couteron, P., Pélissier, R., 2021. Evaluation of automated pipelines for tree and plot metric estimation from TLS data in tropical forest areas. Ann. Bot. 128, 753–766. https://doi.org/10.1093/aob/mcab051

Mitchard, E.T.A., 2018. The tropical forest carbon cycle and climate change. Nature 559, 527–534. https://doi.org/10.1038/s41586-018-0300-2

 doi:10.20944/preprints202603.1717.v1

Molto, Q., Hérault, B., Boreux, J.J., Daullet, M., Rousteau, A., Rossi, V., 2014. Predicting tree heights for biomass estimates in tropical forests -A test from French Guiana. Biogeosciences 11, 3121–3130. https://doi.org/10.5194/bg-11-3121-2014

Molto, Q., Rossi, V., Blanc, L., 2013. Error propagation in biomass estimation in tropical forests. Methods Ecol. Evol. 4, 175–183. https://doi.org/10.1111/j.2041-210x.2012.00266.x

Momo, S.T., Ploton, P., Martin-Ducup, O., Lehnebach, R., Fortunel, C., Sagang, L.B.T., Boyemba, F., Couteron, P., Fayolle, A., Libalah, M., Loumeto, J., Medjibe, V., Ngomanda, A., Obiang, D., Pélissier, R., Rossi, V., Yongo, O., Bocko, Y., Fonton, N., Kamdem, N., Katembo, J., Kondaoule, H.J., Maïdou, H.M., Mankou, G., Mbasi, M., Mengui, T., Mofack, G.I.I., Moundounga, C., Moundounga, Q., Nguimbous, L., Ncham, N.N., Asue, F.O.M., Senguela, Y.P., Viard, L., Zapfack, L., Sonké, B., Barbier, N., 2020. Leveraging Signatures of Plant Functional Strategies in Wood Density Profiles of African Trees to Correct Mass Estimations From Terrestrial Laser Data. Sci. Rep. 10, 1–11. https://doi.org/10.1038/s41598-020-58733-w

Momo Takoudjou, S., Ploton, P., Sonké, B., Hackenberg, J., Griffon, S., de Coligny, F., Kamdem, N.G., Libalah, M., Mofack, G., Le Moguédec, G., Pélissier, R., Barbier, N., 2018. Using terrestrial laser scanning data to estimate large tropical trees biomass and calibrate allometric models: A comparison with traditional destructive approach. Methods Ecol. Evol. 9, 905–916. https://doi.org/10.1111/2041-210X.12933

Muledi, J.I., Momo, S.T., Ploton, P., Kamukenge, A.L., Ibey, W.K., Pamavesi, B.M., Mushabaa, B.A., Shutcha, M.N., Mwenze, D.N., Sonké, B., Tshanika, U.M., Bamuninga, B.T., Ndikumagenge, C., Barbier, N., 2025. Allometric Equations for Aboveground Biomass Estimation in Wet Miombo Forests of the Democratic Republic of the Congo Using Terrestrial LiDAR. Environments 2025, Vol. 12, Page 260 12, 260. https://doi.org/10.3390/ENVIRONMENTS12080260

Ngomanda, A., Engone Obiang, N.L., Lebamba, J., Moundounga Mavouroulou, Q., Gomat, H., Mankou, G.S., Loumeto, J., Midoko Iponga, D., Kossi Ditsouga, F., Zinga Koumba, R., Botsika Bobé, K.H., Mikala Okouyi, C., Nyangadouma, R., Lépengué, N., Mbatchi, B., Picard, N., 2014. Site-specific versus pantropical allometric equations: Which option to estimate the biomass of a moist central African forest? For. Ecol. Manage. 312, 1–9. https://doi.org/10.1016/j.foreco.2013.10.029

Osnas, J.L.D., Lichstein, J.W., Reich, P.B., Pacala, S.W., 2013. Global leaf trait relationships: Mass, area, and the leaf economics spectrum. Science (1979). 340, 741–744. https://doi.org/10.1126/science.1231574

Pan, Y., Birdsey, R.A., Fang, J., Houghton, R., Kauppi, P.E., Kurz, W.A., Phillips, O.L., Shvidenko, A., Lewis, S.L., Canadell, J.G., Ciais, P., Jackson, R.B., Pacala, S.W., McGuire, A.D., Piao, S., Rautiainen, A., Sitch, S., Hayes, D., 2011. A large and persistent carbon sink in the world's forests. Science (1979). 333, 988–993. https://doi.org/10.1126/science.1201609

Ploton, P., Barbier, N., Momo, S.T., Rejou-Mechain, M., Boyemba Bosela, F., Chuyong, G., Dauby, G., Droissart, V., Fayolle, A., Calisto Goodman, R., Henry, M., Guy Kamdem, N., Katembo Mukirania, J., Kenfack, D., Libalah, M., Ngomanda, A., Rossi, V., Sonke, B., Texier, N., Thomas, D., Zebaze, D., Couteron, P., Berger, U., Pélissier, R., 2016. Closing a gap in tropical forest biomass estimation: Taking crown mass variation into account in pantropical allometries. Biogeosciences 13, 1571–1585. https://doi.org/10.5194/bg-13-1571-2016

Poorter, H., Jagodzinski, A.M., Ruiz-peinado, R., Kuyah, S., Luo, Y., Oleksyn, J., Usoltsev, V.A., Buckley, T.N., Reich, P.B., Sack, L., 2015. How does biomass distribution change with size and differ among species ? An analysis for 1200 plant species from five continents.

Poorter, L., Bongers, L., Bongers, F., 2006. Architecture of 54 moist-forest tree species: Traits, trade-offs, and functional groups. Ecology 87, 1289–1301. https://doi.org/10.1890/0012-9658(2006)87[1289:AOMTST]2.0.CO;2

Proulx, H., Jacobs, J.M., Burakowski, E.A., Cho, E., Hunsaker, A.G., Sullivan, F.B., Palace, M., Wagner, C., 2022. Comparison of in-situ snow depth measurements and impacts on validation of unpiloted aerial system lidar over a mixed-use temperate forest landscape. https://doi.org/10.5194/TC-2022-7

R Core Team, 2025. A Language and Environment for Statistical Computing.

Raumonen, P., Casella, E., Calders, K., Murphy, S., Åkerbloma, M., Kaasalainen, M., 2015. Massive-Scale Tree Modelling From Tls Data. ISPRS Annals of Photogrammetry, Remote Sensing and Spatial Information Sciences II-3/W4, 189–196. https://doi.org/10.5194/isprsannals-II-3-W4-189-2015

 doi:10.20944/preprints202603.1717.v1

Raumonen, P., Kaasalainen, M., Åkerblom, M., Kaasalainen, S., Kaartinen, H., Vastaranta, M., Holopainen, M., Disney, M., Lewis, P., 2013. Fast Automatic Precision Tree Models from Terrestrial Laser Scanner Data. Remote Sens. (Basel). 5, 491–520. https://doi.org/10.3390/rs5020491

Raumonen, P., Kaasalainen, S., Kaasalainen, M., Kaartinen, H., 2012. Approximation of Volume and Branch Size Distribution of Trees From Laser Scanner Data. ISPRS - International Archives of the Photogrammetry, Remote Sensing and Spatial Information Sciences XXXVIII-5/, 79–84. https://doi.org/10.5194/isprsarchives-XXXVIII-5-W12-79-2011

Réjou-Méchain, M., Barbier, N., Couteron, P., Ploton, P., Vincent, G., Herold, M., Mermoz, S., Saatchi, S., Chave, J., Boissieu, F. de, Férêt, J.-B., Momo Takoudjou, S., Pélissier, R., 2019. Upscaling forest biomass from field to satellite measurements: sources of errors and ways to reduce them, Surveys in Geophysics. Springer Netherlands. https://doi.org/10.1007/s10712-019-09532-0

Réjou-Méchain, M., Mortier, F., Bastin, J.F., Cornu, G., Barbier, N., Bayol, N., Bénédet, F., Bry, X., Dauby, G., Deblauwe, V., Doucet, J.L., Doumenge, C., Fayolle, A., Garcia, C., Kibambe Lubamba, J.P., Loumeto, J.J., Ngomanda, A., Ploton, P., Sonké, B., Trottier, C., Vimal, R., Yongo, O., Pélissier, R., Gourlet-Fleury, S., 2021. Unveiling African rainforest composition and vulnerability to global change. Nature 593, 90–94. https://doi.org/10.1038/s41586-021-03483-6

Sagang, L.B.T., Favrichon, S., Dalagnol, R., Ordway, E.M., Medjibe, V., Manfoumbi, F., Obame, C., Wagner, F., George-Chacon, S., White, L., Saatchi, S., 2024. Unveiling spatial variations of high forest live biomass carbon stocks of Gabon using advanced remote sensing techniques. Environmental Research Letters 19, 74038. https://doi.org/10.1088/1748-9326/ad5572

Salis, S.M., Assis, M.A., Mattos, P.P., Pião, A.C.S., 2006. Estimating the aboveground biomass and wood volume of savanna woodlands in Brazil's Pantanal wetlands based on allometric correlations. For. Ecol. Manage. 228, 61–68. https://doi.org/10.1016/j.foreco.2006.02.025

Schepaschenko, D., Chave, J., Phillips, O.L., Lewis, S.L., Davies, S.J., Réjou-Méchain, M., Sist, P., Scipal, K., Perger, C., Herault, B., Labrière, N., Hofhansl, F., Affum-Baffoe, K., Aleinikov, A., Alonso, A., Amani, C., Araujo-Murakami, A., Armston, J., Arroyo, L., Ascarrunz, N., Azevedo, C., Baker, T., Bałazy, R., Bedeau, C., Berry, N., Bilous, A.M., Bilous, S.Y., Bissiengou, P., Blanc, L., Bobkova, K.S., Braslavskaya, T., Brienen, R., Burslem, D.F.R.P., Condit, R., Cuni-Sanchez, A., Danilina, D., del Castillo Torres, D., Derroire, G., Descroix, L., Sotta, E.D., D'Oliveira, M.V.N., Dresel, C., Erwin, T., Evdokimenko, M.D., Falck, J., Feldpausch, T.R., Foli, E.G., Foster, R., Fritz, S., Garcia-Abril, A.D., Gornov, A., Gornova, M., Gothard-Bassébé, E., Gourlet-Fleury, S., Guedes, M., Hamer, K.C., Susanty, F.H., Higuchi, N., Coronado, E.N.H., Hubau, W., Hubbell, S., Ilstedt, U., Ivanov, V. V., Kanashiro, M., Karlsson, A., Karminov, V.N., Killeen, T., Koffi, J.C.K., Konovalova, M., Kraxner, F., Krejza, J., Krisnawati, H., Krivobokov, L. V., Kuznetsov, M.A., Lakyda, I., Lakyda, P.I., Licona, J.C., Lucas, R.M., Lukina, N., Lussetti, D., Malhi, Y., Manzanera, J.A., Marimon, B., Junior, B.H.M., Martinez, R.V., Martynenko, O. V., Matsala, M., Matyashuk, R.K., Mazzei, L., Memiaghe, H., Mendoza, C., Mendoza, A.M., Moroziuk, O. V., Mukhortova, L., Musa, S., Nazimova, D.I., Okuda, T., Oliveira, L.C., Ontikov, P. V., Osipov, A.F., Pietsch, S., Playfair, M., Poulsen, J., Radchenko, V.G., Rodney, K., Rozak, A.H., Ruschel, A., Rutishauser, E., See, L., Shchepashchenko, M., Shevchenko, N., Shvidenko, A., Silveira, M., Singh, J., Sonké, B., Souza, C., Stereńczak, K., Stonozhenko, L., Sullivan, M.J.P., Szatniewska, J., Taedoumg, H., ter Steege, H., Tikhonova, E., Toledo, M., Trefilova, O. V., Valbuena, R., Gamarra, L.V., Vasiliev, S., Vedrova, E.F., Verhovets, S. V., Vidal, E., Vladimirova, N.A., Vleminckx, J., Vos, V.A., Vozmitel, F.K., Wanek, W., West, T.A.P., Woell, H., Woods, J.T., Wortel, V., Yamada, T., Nur Hajar, Z.S., Zo-Bi, I.C., 2019. The Forest Observation System, building a global reference dataset for remote sensing of forest biomass. Sci. Data 6, 1–11. https://doi.org/10.1038/s41597-019-0196-1

Sirri, N.F., Libalah, M.B., Momo Takoudjou, S., Ploton, P., Medjibe, V., Kamdem, N.G., Mofack, G., Sonké, B., Barbier, N., 2019. Allometric Models to Estimate Leaf Area for Tropical African Broadleaved Forests. Geophys. Res. Lett. 46, 8985–8994. https://doi.org/10.1029/2019GL083514

Siyum, Z.G., 2020. Tropical dry forest dynamics in the context of climate change: syntheses of drivers, gaps, and management perspectives. Ecol. Process. 9. https://doi.org/10.1186/s13717-020-00229-6

 doi:10.20944/preprints202603.1717.v1

Terryn, L., Calders, K., Åkerblom, M., Bartholomeus, H., Disney, M., Levick, S., Origo, N., Raumonen, P., Verbeeck, H., 2023. Analysing individual 3D tree structure using the R package ITSMe. Methods Ecol. Evol. 14, 231–241. https://doi.org/10.1111/2041-210X.14026

Terryn, L., Calders, K., Disney, M., Origo, N., Malhi, Y., Newnham, G., Raumonen, P., Å kerblom, M., Verbeeck, H., 2020. Tree species classification using structural features derived from terrestrial laser scanning. ISPRS Journal of Photogrammetry and Remote Sensing 168, 170–181. https://doi.org/10.1016/j.isprsjprs.2020.08.009

Tian, Z., Li, S., 2022. Graph-Based Leaf-Wood Separation Method for Individual Trees Using Terrestrial Lidar Point Clouds. IEEE Transactions on Geoscience and Remote Sensing 60. https://doi.org/10.1109/TGRS.2022.3218603

Vandendaele, B., Martin-Ducup, O., Fournier, R.A., Pelletier, G., 2024. Evaluation of mobile laser scanning acquisition scenarios for automated wood volume estimation in a temperate hardwood forest using quantitative structural models. Canadian Journal of Forest Research. https://doi.org/10.1139/cjfr-2023-0202

Vandendaele, B., Martin-Ducup, O., Fournier, R.A., Pelletier, G., Lejeune, P., 2022. Mobile Laser Scanning for Estimating Tree Structural Attributes in a Temperate Hardwood Forest. Remote Sens. (Basel). 14, 4522. https://doi.org/10.3390/RS14184522

Verbeeck, H., Bauters, M., Jackson, T., Shenkin, A., Disney, M., Calders, K., 2019. Time for a Plant Structural Economics Spectrum. Frontiers in Forests and Global Change 2, 1–5. https://doi.org/10.3389/ffgc.2019.00043

Vicari, Matheus B., Disney, M., Wilkes, P., Burt, A., Calders, K., Woodgate, W., 2019. Leaf and wood classification framework for terrestrial LiDAR point clouds. Methods Ecol. Evol. 10, 680–694. https://doi.org/10.1111/2041-210X.13144

Vicari, Matheus Boni, Pisek, J., Disney, M., 2019. New estimates of leaf angle distribution from terrestrial LiDAR: Comparison with measured and modelled estimates from nine broadleaf tree species. Agric. For. Meteorol. 264, 322–333. https://doi.org/10.1016/J.AGRFORMET.2018.10.021

Wang, D., Momo Takoudjou, S., Casella, E., 2020. LeWoS: A universal leaf-wood classification method to facilitate the 3D modelling of large tropical trees using terrestrial LiDAR. Methods Ecol. Evol. 11, 376–389. https://doi.org/10.1111/2041-210X.13342

White, F., 1983. The vegetation of Africa.

Wilkes, P., Disney, M., Armston, J., Bartholomeus, H., Bentley, L., Brede, B., Burt, A., Calders, K., Chavana-Bryant, C., Clewley, D., Duncanson, L., Forbes, B., Krisanski, S., Malhi, Y., Moffat, D., Origo, N., Shenkin, A., Yang, W., 2023. TLS2trees: A scalable tree segmentation pipeline for TLS data. Methods Ecol Evol 14, 3083–3099. https://doi.org/10.1111/2041-210X.14233

Wright, I.J., Reich, P.B., Westoby, M., Ackerly, D.D., Baruch, Z., Bongers, F., Cavender-Bares, J., Chapin, T., Cornellssen, J.H.C., Diemer, M., Flexas, J., Garnier, E., Groom, P.K., Gulias, J., Hikosaka, K., Lamont, B.B., Lee, T., Lee, W., Lusk, C., Midgley, J.J., Navas, M.L., Niinemets, Ü., Oleksyn, J., Osada, H., Poorter, H., Pool, P., Prior, L., Pyankov, V.I., Roumet, C., Thomas, S.C., Tjoelker, M.G., Veneklaas, E.J., Villar, R., 2004. The worldwide leaf economics spectrum. Nature 428, 821–827. https://doi.org/10.1038/nature02403

Zanne, A.E., Lopez-Gonzalez, G., Coomes, D.A.A., Ilic, J., Jansen, S., Lewis, S.L.S.L., Miller, R.B.B., Swenson, N.G.G., Wiemann, M.C.C., Chave, J., 2009. Data from: Towards a worldwide wood economics spectrum. Dryad Digital Repository. Dryad. https://doi.org/10.5061/dryad.234